Estimator design for a moving bed gasification reactor

Ulises Badillo-Hernández*, Isrrael Nájera*, Jesús Álvarez * and Luis A. Álvarez-Icaza**

** Departamento de Ingeniería de Procesos e Hidráulica,*
Universidad Autónoma Metropolitana-Iztapalapa, Apdo. 55534, 09340 México, D.F. México
*** Instituto de Ingeniería,*
Universidad Nacional Autónoma de México, 04510 México D.F., México

Abstract: The problem of estimating the effluent concentrations of a spatially distributed tubular biomass gasification reactor with a temperature measurement is addressed. The reactor is described by a set of nonlinear partial differential equations (PDEs), and exhibits steady-state multiplicity. First, an $\boldsymbol{N}$-stage (discrete) model that approximates, up to transport-kinetics parameter error, the behavior of the PDE system is built. Then, the application of the geometric estimation approach for staged systems yields a nonlinear robustly convergent estimator with: (i) systematic construction, and (ii) simple tuning procedure for the gain-stage number pair $(\boldsymbol{k_e}, \boldsymbol{N_e})$. The time-varying profiles of the startup operation can be adequately and efficiently estimated with: (i) a staged model of $\boldsymbol{N_e = 8}$ stages, and (ii) a sensor located at the axial position with largest temperature slope change.

Keywords: gasification reactor, detectable estimation structure, geometric estimator.

1. INTRODUCTION

Biomass gasification reactors enable disposal of waste materials with efficient generation of energy in synthetic gaseous (syngas) fuel form (Malkow, 2004). According to experimental (Milligan, 1994; Shwe, 2004) and dynamic partial differential equation (PDE) numerical simulation (Di Blasi, 2000; Ranzi, 2014) studies the ignition-type steady-state (SS) of interest (with largest effluent caloric concentration) is accompanied by an undesirable extinction steady-state. The complexity of the dynamics is due to the spatial coupling of an exothermic chemical reaction network with mass-heat transport. The reaction network includes heterogeneous pyrolysis, char combustion and water-shift reactions. The transport phenomena include convective mass and convective-dispersive-radiative heat mechanisms. Such reactor behavior: (i) corresponds to a complex global-nonlinear dynamics, with phenomena (such as multiplicity, bifurcation and limit cycling) that cannot be described by a local dynamical framework, and (ii) is commonly modelled with a set of nonlinear PDEs (Gobel, 2007) made by dynamic and quasi-static components (Badillo-Hernández et. al. 2013).

Recently, Badillo-Hernandez et al. 2016 with continuation-bifurcation analysis established that: (i) the syngas reactor has three SSs in classic configuration (the ignition SS of interest, an extinction stable SS, and an unstable saddle SS in between), (ii) according to the cell modeling approach (Deans & Lapidus, 1960; Levenspiel, 1962; Deckwer, 1974; Nájera, 2016), the global-nonlinear dynamics can be quantitatively described, up the uncertainty of the PDE model with typical parameter error, with a low-order N_q-stage model (the continuous, shutdown, and startup operations can be described with N_q =12, 12 and 20 stages, respectively), and (iii) to prevent the presence of spurious SSs (due to excessive discretization (Varma, 1980), the stage number had to be chosen above a lower limit N^-.

By far, the nonlinear extended Kalman filter (EKF) has been the most widely used and tested estimation technique in chemical process (Kazantzis & Kravaris, 2000). Due to its high-dimensionality drawback, the EKF for gasification tubular reactors has been implemented on the basis of oversimplified reduced models (Wilson, 2006), with questionably functioning beyond a small locality. Instead, the estimation task has been pursued for a fluidized bed gasifier using a single CSTR model (Botero et. al. 2013) and applying the so-called asymptotic observer technique (Dochain, et. al. 1992) which amounts to running the open-loop model with the measured state replaced by the actual measurement. Due to the need of computing high-order Lie derivatives, the application of high-gain and nonlinear Luenberger-like observers (Zeitz 1987; Ciccarella et al 1993; Gauthier et al 1992) for staged finite-dimensional systems is an intractable task. The dimensionality problems for injection-based estimators have been overcome in the context of large-dimensional (from 200 to 400 states) laboratory and industrial multicomponent staged distillation columns (Fernandez et. al., 2012, Porru et. al. 2013) by means of the nonlinear geometric estimation approach for staged systems (Alvarez and Fernandez, 2009; Fernandez et. al., 2012).

These considerations motivate the present study on the staged model-based estimation problem of a spatially distributed syngas reactor with complex global-nonlinear dynamics. Specifically, the objective is to estimate the effluent concentrations on the basis of an N_e-stage model (with N_e to be precised) in conjunction with: (i) gas and solid feed flow input $\boldsymbol{u}$, and (i) output temperature measurement (y) located at the sensitive location (entrance: $0 < z_y < 1$: exit, where the temperature slope change is maximum) that is commonly employed for temperature control of industrial exothermic packed-bed tubular reactors (Bashir et. al., 1992).

Firstly (in Section 2), the estimation problem is stated. Secondly (in Section 3), the results by Badillo-Hernandez et. al. 2016 are recalled to set the staged model for estimation. Thirdly (in Section 4), the reactor nonlinear estimator is designed according to the geometric estimation approach for staged systems (Alvarez and Fernandez, 2009; Fernandez et. al., 2012). Finally (in Section 5), the conclusions are stated.

2. ESTIMATION PROBLEM

2.1 Syngas tubular moving bed reactor

Regard downdraft continuous bed tubular gasification reactor of length L, transversal area A and total metal mass m_w (depicted in Figure 1) where solid (s) and gas (g) reactants are fed at the top and converted into syngas and biochar products. The solid is fed at mass flow M_{se}, component densities vector $\boldsymbol{\rho}_{se}$, temperature T_{se} and with a particle size d_{pe}. The gas is fed at volumetric rate Q_{ge}, concentration vector $\boldsymbol{C}_{ge}$, and temperature T_{ge}. The effluent gas has volumetric rate Q_{gf}, concentration vector $\boldsymbol{C}_{gf}$, and temperature T_{gf}.

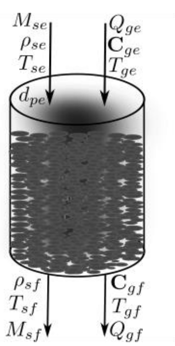

Fig. 1. Downdraft syngas tubular moving bed reactor.

The effluent ash and char stream has mass flow M_{sf}, density vector $\boldsymbol{\rho}_{sf}$, and temperature T_{sf}. The sets of solid ($\mathcal{S}_s$) and gas phase ($\mathcal{S}_g$) chemical species are

$$\mathcal{S}_s = \{B, C\}, \quad \mathcal{S}_g = \{O_2, H_2, CO, CO_2, H_2O, CH_4, Tars, N_2\}$$

Under the standard assumptions of quasi-static (QSS) gas phase dynamics, large interphase heat transport (Hlavacek, 1970) and spatial homogeneity the syngas reactor is described by the partial differential equations (PDEs) in dimensionless form (Badillo-Hernandez et al. 2013, 2016):

$$0 \approx -\partial_z[v_g c_G(\tau)] + \boldsymbol{m}^T\boldsymbol{r}(\boldsymbol{c},\tau) \quad (1a)$$
$$0 = c_{C0}\partial_z v_s + W_{ab}[r_2(\boldsymbol{c},\tau) + r_3(\boldsymbol{c},\tau) + r_4(\boldsymbol{c},\tau)] \quad (1b)$$
$$0 \approx -\partial_z[v_g \boldsymbol{c}_g] + \boldsymbol{S}_g\boldsymbol{r}(\boldsymbol{c},\tau) \quad (1c)$$
$$\partial_t \boldsymbol{c}_s = -\partial_z[v_s\boldsymbol{c}_s] + W_{ab}\boldsymbol{S}_s\boldsymbol{r}(\boldsymbol{c},\tau) \quad (1d)$$
$$\partial_t\tau = h_T^{-1}(\boldsymbol{c_s})\{\partial_z[\delta\,\kappa(\tau)\partial_z\tau - v_h(\boldsymbol{v},\boldsymbol{c},\tau)\tau] \quad (1e)$$
$$\partial_z[h_T(\boldsymbol{c_s})v_s]\tau - \upsilon(\tau)[\tau - \tau_c(t)] + W_{ab}\boldsymbol{\Delta}^T\boldsymbol{r}(\boldsymbol{c},\tau)\} \quad (1f)$$
$$y = \tau(z_y,t), \;\; 0 < z_y < 1, \;\; \partial_{zz}^2\bar{\tau}(z_y) \approx 0 \quad (1g)$$

with boundary and initial conditions

$$z = 0{:}\, \boldsymbol{c}_\pi(0,t) = \boldsymbol{c}_{\pi e}(t),\, v_\pi(0,t) = v_{\pi e}(t), \;\pi = s, g$$
$$\delta\kappa(\tau)\partial_z\tau = v_h(\boldsymbol{c},\tau)[\tau - \tau_e(t)] \quad (1f)$$
$$z = 1{:}\, \partial_z\tau = 0, \; t = 0{:}\, \boldsymbol{c}_s(z,0) = \boldsymbol{c}_{so}(z), \tau(z,0) = \tau_o(z) \quad (1g)$$

where

$$\boldsymbol{c} = (\boldsymbol{c}_s^T, \boldsymbol{c}_g^T)^T, \quad \boldsymbol{c}_s = (c_1^s, c_2^s)^T, \quad \boldsymbol{c}_g = (c_1^g, \dots, c_8^g)^T$$
$$\boldsymbol{r}(\boldsymbol{c},\tau) = (r_1, \dots, r_{n_R})^T(\boldsymbol{c},\tau), \qquad \boldsymbol{\Delta}^T = (\Delta_1, \dots, \Delta_{n_R})^T$$
$$h_T(\boldsymbol{c_s}) \approx c_{pS}c_S(\boldsymbol{c_s}), \quad \kappa(\tau) = \frac{K(T_r)}{K(T)}, \quad \delta = 1/Pe$$
$$\upsilon(\tau) = St_w\mu(\tau), \qquad St_w = \frac{Lh_w(T_r)}{H_{sr}V_{sr}}, \quad \mu(\tau) = \frac{h_w(T_r\tau)}{h_w(T_r)}$$
$$v_h(\boldsymbol{v},\boldsymbol{c},\tau) = W_{ab}v_g c_{pG}c_G(\boldsymbol{c},\tau) + v_s c_{pS}c_S(\boldsymbol{c}_s), \; \boldsymbol{v} = (v_s, v_g)^T$$

Eq. (1a-b) is the quasi-static (QS) version of the parasitic robustly stable gas concentration-temperature dynamics, t is the time, z the axial position, τ the temperature, and c_i^s (or c_i^g) the concentration of the i-th component in the solid (or gas) phase, v_g (or v_s) is the dimensionless solid (or gas) velocity, and y is the temperature measurement at the axial location z_y, with largest slope change, of industrial temperature controllers (Bashir et al., 1992).

In eq. (1), v_h is the effective heat convective flux, κ is the effective thermal conductivity of the bed, c_G and c_{pG} (or c_S and , c_{pS}) are the total molar concentration and specific heat capacity of gas (or solid) phase, $\boldsymbol{S}_s$ (or $\boldsymbol{S}_g$) is the stoichiometric submatrix of the solid (or gas) phase, $\boldsymbol{r}$ (or $\boldsymbol{\Delta}$) is the vector with $n_R = 8$ reaction rates r_i (or heats of reaction Δ_i), μ is the wall heat transfer coefficient, and δ is the heat dispersion number (inverse of the Peclet number Pe). The model parameters, including densities, kinetics and transport parameters are the ones employed in previous simulation studies (Di Blasi 2000, Badillo-Hernandez et al. 2013). In particular, the length-to-particle diameter quotient (N^+) and heat dispersion (inverse Peclet) number (δ) are:

$$\mathrm{N}^+ = L/d_p = 50, \qquad \delta = 1/6 \quad (2)$$

According to previous experimental and simulation studies (Milligan, 1994; Shwe, 2004, Ranzi et. al., 2014, Badillo-Hernandez et al. 2016), the syngas reactor exhibits complex behavior with three steady-state (SS) profile sets $[\bar{\boldsymbol{c}}(z), \bar{\tau}(z), \bar{\boldsymbol{v}}(z)]_{i=1,2,3}$ with a structure that is classic in chemical reactor engineering (Amundson, 1980): two stable steady-states (SS_3 and SS_1) with un unstable saddle (SS_1) in between. The SSs SS_1 and SS_3 correspond to (low-temperature) extinction and (high-temperature) ignition regimes, respectively. In the syngas reactor, the ignition SS SS_3, with largest energy efficieny production, is the one of interest. In other words, the reactor must be robustly operated about the high-temperature ignition open-loop locally stable SS SS_3.

Following the standard simulation procedures, the PDE set (1) was solved numerically by means of finite differences with $N_{fd} = 200$ nodes (Di Blasi 2000). In Fig. 2 are presented a sample of the temperature (T), gas flow (q_g), hydrogen concentration (X_{H_2}), and carbon dioxide concentration (X_{CO_2}) SS profiles: (i) extinction SS_1 (continuous curves 1), (ii) unstable saddle SS_2 (discontinuous pink curves 2), and (iii) ignition SS_3 (continuous curves 3) recalled from Badillo-Hernandez et al. 2016.

2.2 Problem

Our problem consists in estimating the temperature and concentration effluents of the syngas packed bed tubular reactor (1): (i) on the basis of an n_e*-finite dimensional model* and the feed flow rate pair ($\boldsymbol{u}$) as well as the output temperature (y) *measurements*, and (ii) by means of a robustly convergent nonlinear geometric (G) state estimator (Alvarez and Fernandez, 2009) for N-staged systems

(Fernandez et. al. 2012). The aim is to draw an estimator with: (i) the least possible number n_e of ordinary differential equations (ODEs), (ii) systematic construction, and (iii) simple procedure to tune the gain-stage number pair $(\boldsymbol{k_e}, N_e)$.

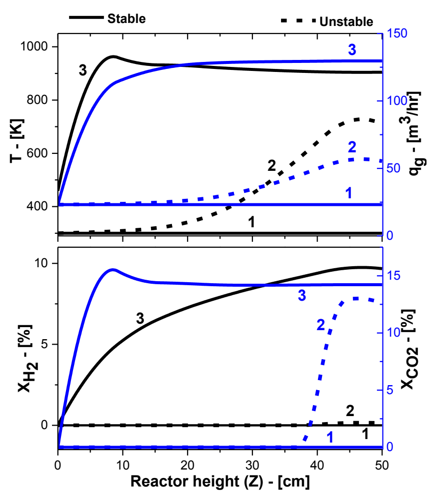

Fig. 2. Reactor stable extinction SS_1 (1), unstable saddle SS_2 (2), and stable ignition SS_3 (3) SS profiles: (i) temperature (T), and gas flow (q_g), and (ii) hydrogen (X_{H2}) and carbon dioxide (X_{CO2}) concentrations.

The estimator functioning will be tested through numerical simulation with the *transient start-up*: from an extinction initial state to the ignition SS_3. By doing so, the observer will be subjected to a severe test, as the distributed reactor evolves in an ample region of its state space.

3. STAGED MODEL

In this section, developments and results in (Badillo-Hernandez et. al. 2013, 2016) on the approximation of the PDE reactor model (1) with a low-dimensional N-staged model are recalled with one important consideration: here the stage number N becomes a design degree of freedom.

Following the developments and results in (Badillo-Hernandez et. al. 2016), the spatial discretization through *finite differences* (over a uniform mesh with N domain points) of the PDE model (1) yields the *N-stage reactor model*

$$0 = \boldsymbol{\varphi}_\chi(\boldsymbol{\chi}, \boldsymbol{x}_c, \boldsymbol{x}_\tau, \boldsymbol{u}) \tag{3a}$$

$$\dot{\boldsymbol{x}}_c = \boldsymbol{\varphi}_c(\boldsymbol{\chi}, \boldsymbol{x}_c, \boldsymbol{x}_\tau, \boldsymbol{u}), \quad \boldsymbol{x}_c(0) = \boldsymbol{x}_{co} \tag{3b}$$

$$\dot{\boldsymbol{x}}_\tau = \boldsymbol{\varphi}_\tau(\boldsymbol{\chi}, \boldsymbol{x}_c, \boldsymbol{x}_\tau, \boldsymbol{u}), \quad \boldsymbol{x}_\tau(0) = \boldsymbol{x}_{\tau o}, \quad y = \boldsymbol{c}_y \boldsymbol{x}_\tau \tag{3c}$$

where

$$y = \boldsymbol{c}_y \boldsymbol{x}_\tau = \tau(z_y, t), \quad 0 < z_y < 1, \quad \partial_{zz}^2 \bar{\tau}(z_y) \approx 0 \tag{3d}$$

$$\boldsymbol{x_c} = (\boldsymbol{c}_{s,1}^T, \dots, \boldsymbol{c}_{s,N}^T)^T, \quad \dim \boldsymbol{x_c} = n_s N \coloneqq n_c$$

$$\boldsymbol{x}_\tau = (\tau_1, \dots, \tau_N)^T, \quad \dim \boldsymbol{x}_\tau = N \coloneqq n_\tau$$

$$\boldsymbol{x} = (\boldsymbol{x}_1^T, \dots, \boldsymbol{x}_N^T)^T, \boldsymbol{x}_i = (\boldsymbol{c}_{si}^T, \tau_i)^T, dim\, \boldsymbol{x} = N(n_s + 1) \coloneqq n_x$$

$\boldsymbol{x}$ is the dynamic state, $\boldsymbol{\chi}$ is the quasi-static (QS) state, eq. (3a) is the QS version of the parasitic robustly stable gas concentration-temperature dynamics, $\boldsymbol{x}_i$ (or $\boldsymbol{\chi}_i$) contains the entries of $\boldsymbol{x}$ (or $\boldsymbol{\chi}$) at the i-th stage, y is the output temperature measurement, and $\boldsymbol{u}$ is the known or measured input vector with the volumetric feed flows vector $(\boldsymbol{v}_e A)$, concentrations $(\boldsymbol{c}_{se}, \boldsymbol{c}_{ge})$, and temperature ($\tau_e$ and τ_a).

The substitution in the ODEs (3b-c) of the solution for $\boldsymbol{\chi}$ of the algebraic system (3a) yields the N-stage model (4)

$$\dot{\boldsymbol{x}}_c = \boldsymbol{f}_c(\boldsymbol{x}_c, \boldsymbol{x}_\tau, \boldsymbol{u}), \quad \boldsymbol{x}_c(0) = \boldsymbol{x}_{co} \tag{4a}$$

$$\dot{\boldsymbol{x}}_\tau = \boldsymbol{f}_\tau(\boldsymbol{x}_c, \boldsymbol{x}_\tau, \boldsymbol{u}), \quad \boldsymbol{x}_\tau(0) = \boldsymbol{x}_{\tau o}, \quad y = h_y(\boldsymbol{x}_\tau) \tag{4b}$$

$$\boldsymbol{\chi} = \boldsymbol{f}_\chi(\boldsymbol{x}_c, \boldsymbol{x}_\tau, \boldsymbol{u}), \quad y = h_y(\boldsymbol{x}_\tau) \tag{4c}$$

in standard input-state output form, where

$\boldsymbol{\chi} = \boldsymbol{f}_\chi(\boldsymbol{x}_c, \boldsymbol{x}_\tau, \boldsymbol{u})$: unique solution for $\boldsymbol{\chi}$ of eq. (3a)

$$\boldsymbol{f}_\tau(\boldsymbol{x}_c, \boldsymbol{x}_\tau, \boldsymbol{u}) = \boldsymbol{\varphi}_\tau[\boldsymbol{g}(\boldsymbol{x}_c, \boldsymbol{x}_\tau, \boldsymbol{u}), \boldsymbol{x}_c, \boldsymbol{x}_\tau, \boldsymbol{u}]$$

$$\boldsymbol{f}_c(\boldsymbol{x}_c, \boldsymbol{x}_\tau, \boldsymbol{u}) = \boldsymbol{\varphi}_c[\boldsymbol{g}(\boldsymbol{x}_c, \boldsymbol{x}_\tau, \boldsymbol{u}), \boldsymbol{x}_c, \boldsymbol{x}_\tau, \boldsymbol{u}]$$

In compact form, the *N-stage reactor model* (4) is written as

$$\dot{\boldsymbol{x}} = \boldsymbol{f}(\boldsymbol{x}, \boldsymbol{u}), \quad \boldsymbol{x}(0) = \boldsymbol{x}_o, \quad \dim \boldsymbol{x} = n = 3N \tag{5a}$$

$$\boldsymbol{\chi} = \boldsymbol{g}(\boldsymbol{x}, \boldsymbol{u}), \quad y = h(\boldsymbol{x}), \quad n^- \le n \le n_q \le n^+ \tag{5b}$$

where

$$9 = N^- \le N \le N_q = 20 \le N^+ = 50 < N_{fe} \approx 200 \tag{5c}$$

$$27 = n^- \le n \le n_q = 60 \le n^+ = 150 \tag{5d}$$

$$\boldsymbol{x} = (\boldsymbol{x}_c', \boldsymbol{x}_\tau')', \quad \boldsymbol{g}(\boldsymbol{x}, \boldsymbol{u}) = \boldsymbol{f}_\chi(\boldsymbol{x}_c, \boldsymbol{x}_\tau, \boldsymbol{u}) \tag{5e}$$

$$\boldsymbol{f}(\boldsymbol{x}, \boldsymbol{u}) = [\boldsymbol{f}_\tau'(\boldsymbol{x}_c, \boldsymbol{x}_\tau, \boldsymbol{u}), \boldsymbol{f}_\tau'(\boldsymbol{x}_c, \boldsymbol{x}_\tau, \boldsymbol{u})]' \tag{5f}$$

According to the developments in (Badillo-Hernandez et. al. 2013, 2016): $N^- = 9$ is the minimum number of stages required to robustly-qualitatively describe the reactor bistability property (with preclusion of spurious SSs), $N_q = 20$ is the number of stages needed to quantitatively describe the reactor dynamics. N_{fe} is the number of staged employed before to numerically solve the reactor PDE equations (1) (Di Blasi, 2000).

3.1 Model robustness

In Badillo-Hernandez et. al. (2016) with bifurcation analysis (Kuznetsov, 1998; Dhooge, et. al. 2003), the syngas N-stage model dynamics (4) over the heat dispersion-stage number has been characterized, for the parameter space. Here, salient features relevant for the estimator design problem are discussed.

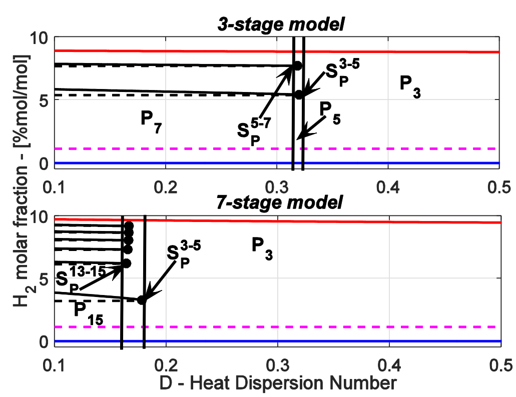

Fig. 3. Change of effluent hydrogen concentration $X_{H2,N}$ with the heat dispersion number δ for $N = 3$ (top) and $N = 7$ (botttom) stages with dependency of multiplicity on δ.

In Fig. 3 is presented the change of effluent hydrogen concentration with the heat dispersion number δ for $N = 3$ and $N = 7$ stages, showing that: (i) for $N = 3$, the staged model has dispersion intervals with 3 (no spurious SSs), 5 (2 spurious SSs) and 7 (4 spurious SSs) SS's, and (ii) for $N = 7$, the model has dispersion intervals with 3 (no spurious SSs), 5 (2 spureous SSs), 7… up to 15 (12 spurious SSs) SS's. This illustrates the phenomena of *spurious SS generation* by excessive discretization of the exothermic tubular reactor of gasification (Varma, 1980).

In Fig. 4 are presented the interpolated temperature SS profiles of the model with $N = 7$ stages, for heat dispersions $\delta = 0.2$ (top) and 0.17 (center), as well as $N = 3$ for $\delta = 0.17$ (bottom).

For fixed number $N = 7$ of stages (top and center panels of Fig. 4), there are 3 SSs (the actual ones) in classic configuration when $\delta = 0.2$ (top panel), and there are 5 SSs (the actual ones plus two spurious SSs) when $\delta = 0.17$ (center panel). This means that the staged model with $(\delta, N) = (0.2,7)$ has *fragile dynamics* in the standard sense of structural instability (Andronov and Pontryagin, 1937) with respect to the heat transport parameter δ: a small change in δ produces a qualitative change (creation or destruction of two SSs by saddle-node bifurcation) in the dynamics.

For fixed heat dispersion number at a typical value $\delta = 0.17$ (center and bottom panels of Fig. 4), there are 5 SSs for $N = 7$ (the 3 actual ones of Figure 2 plus 2 spurious SSs) (center panel of Fig. 4), and for $N = 3$ are 7 SSs (the 3 actual ones of Figure 2 plus 4 spurious SSs) (bottom panel of Fig. 4). This means that the staged model with $(\delta, N) = (0.17,3)$ has *fragile dynamics* by saddle-node bifurcation, in *a nonstandard sense*: with respect to the integer number N of stages of the model dynamics, or equivalently, with respect to the dimensionality of the staged model.

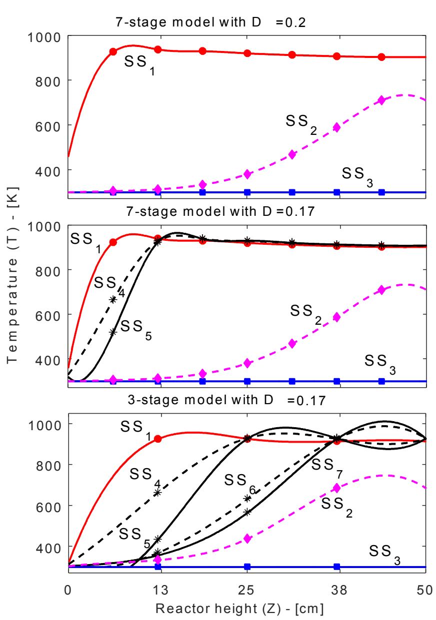

Fig. 4. Interpolated temperature SS profiles of the model with $N = 7$ stages, for heat dispersions $\delta = 0.2$ (top) and 0.17 (center), as well as $N = 3$ for $\delta = 0.17$ (bottom). Structural instability of spurious SSs (black profiles) under changes of N and δ.

These results: (i) explain the lower stage number limit $N^- = 9$ (stated in eq. 5c) for estimator design purposes, for the typical heat dispersion number $\delta = 0.17$ of the present study, in order to robustly describe the actual distributed dynamics with an N-staged model for $N_e > N^- = 9$, and (ii) should be carefully accounted for in the estimator design and testing (section 4).

In order to obtain a quantitatively description of the start-up operation, the number of stages must be increased from $N^- = 9$ to $N_q = 20$ to reduce the discretization error of the staged model (3) to a value comparable to the modeling and experimental errors of the gasifier model (1). Then, the $N_{GE} = N_q = 20$-stage model will be the point of departure to the estimator design carried out in the next section.

3.2 Estimation model with adjustable number of stages

On the basis of the N-stage staged model (5), the model for estimation is given by

$$\dot{\boldsymbol{x}} = \boldsymbol{f}(\boldsymbol{x}, \boldsymbol{u}), \quad \boldsymbol{x}(0) = \boldsymbol{x}_o, \quad \dim \boldsymbol{x} = n = 3N \tag{6a}$$

$$\boldsymbol{\chi} = \boldsymbol{g}(\boldsymbol{x}, \boldsymbol{u}), \quad y = h(\boldsymbol{x}), \quad n \leq n_q \leq n^+ \tag{6b}$$

with

$$N \leq N_q = 20, \quad n \leq n_q = 60 \tag{6c}$$

where: (i) the qualitative-lower (N^-) and quantitative-upper (N_q) limits are fixed, and (ii) the number of stages N is a *design degree of freedom* for the estimator design procedure of the next section. The motion of this system is denoted by

$$\boldsymbol{x}(t) = \boldsymbol{\theta}[\boldsymbol{x_o}, \boldsymbol{u}(t)], \quad \boldsymbol{\theta}[\boldsymbol{x_o}, \boldsymbol{u}(0)] = \boldsymbol{x_o} \tag{7}$$

where $\boldsymbol{\theta}$ is the transition map. Depending on the initial state-input pair $[\boldsymbol{x_o}, \boldsymbol{u}(t)]$, the state $\boldsymbol{x}(t)$ motion can be stable or unstable with robustness or fragile dynamics.

4. NONLINEAR ESTIMATION

In this section the reactor robust estimator is designed with the geometric estimation approach (Alvarez and Fernandez, 2009) for staged systems (Fernandez, et. al. 2012). The aim is to have an estimation error comparable to the N_q-stage model with typical parameter errors.

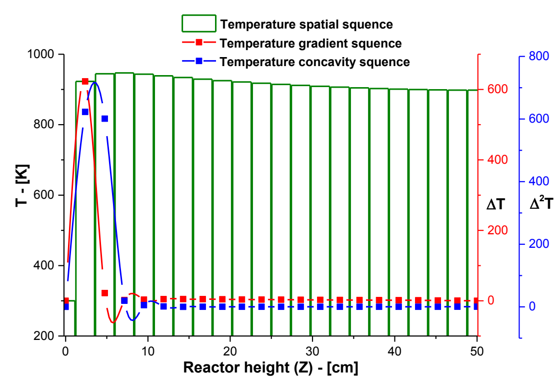

Fig. 5. Temperature SS ignition spatial sequence and its gradient and concavity sequences (and interpolation) of the N-stage model of the syngas reactor, with $N = N_q = 20$.

4.1 Detectability

In Fig. 5 are plotted the SS temperature sequence as well as its gradient and concavity sequences of model (3) with $N_q = 20$ stages. According to the sensitivity criterion for exothermic tubular reactors (Bashir et al., 1992), the temperature measurement must be at stage 1 ($y = \tau_1$).

Thus, consider the motion

$$\boldsymbol{x}^*(t) = \boldsymbol{\theta}^*[\boldsymbol{x}_o^*, \boldsymbol{u}(t), y(t)], \quad \boldsymbol{\theta}^*[\boldsymbol{x}_o^*, \boldsymbol{u}(0), y(0)] = \boldsymbol{x}_o^* \qquad (8)$$

of the $(n-1)$-dimensional dynamical system

$$\dot{\boldsymbol{x}}^* = \boldsymbol{f}(\boldsymbol{x}^*, \boldsymbol{u}), \boldsymbol{x}^*(0) = \boldsymbol{x}_o^*, \ \boldsymbol{x}^*(t) \in X^*(t) \qquad (9a\text{-}b)$$

$$X^*(t) = \{\boldsymbol{x} \in \boldsymbol{R} | h(\boldsymbol{x}) = y(t)\}, \ \dim X^*(t) = n-1 \qquad (9c)$$

that results from the enforcement of the measured output signal $y(t)$ on the N-stage model dynamics (5). When the restricted ($\boldsymbol{x}_o^*$) and non-restricted ($\boldsymbol{x}_o$) initial states coincide, the restricted and actual motions are the same, i.e.,

$$\boldsymbol{x}_o^* = \boldsymbol{x}_o \ \Rightarrow \ \boldsymbol{x}^*(t) = \boldsymbol{x}(t)$$

The motion $\boldsymbol{x}(t)$ of the N-stage system is said to be *robustly (R) detectable* with observability index equal to one (i.e., with passive structure) (Alvarez and Fernandez, 2009) if the motion $\boldsymbol{x}^*(t)$ (8) of the restricted N-stage $(n-1)$-dimensional dynamics (9) robustly converges to the motion $\boldsymbol{x}(t)$ (7) of the unrestricted N-stage n-dimensional dynamics (6), i.e.,

$$\boldsymbol{x}_o^* \neq \boldsymbol{x}_o \ \Rightarrow \ \boldsymbol{x}^*(t) \to \boldsymbol{x}(t) \qquad (10)$$

With numerical simulation it was established that, for measurement at stage 1 and $8 = N^- - 1 \le N \le N_q = 20$ the start-up motion $\boldsymbol{x}(t)$ (7) of the N-stage system (6) is R-stable, meaning that $\boldsymbol{x}(t)$ is *R-detectable*.

4.2 Nonlinear geometric estimator

Given the passive R-detectability property of the N-stage model startup motion $\boldsymbol{x}(t)$ (7), the corresponding R-convergent geometric estimator (Fernandez, et. al. 2012) for the syngas tubular reactor (1) is:

$$\dot{\hat{\boldsymbol{x}}}_c = \boldsymbol{f}_c(\hat{\boldsymbol{x}}_c, \hat{\boldsymbol{x}}_\tau, \boldsymbol{u}), \qquad \hat{\boldsymbol{x}}_c(0) = \hat{\boldsymbol{x}}_{co} \quad (11a)$$

$$\dot{\hat{\boldsymbol{x}}}_\tau = \boldsymbol{f}_\tau(\hat{\boldsymbol{x}}_c, \hat{\boldsymbol{x}}_\tau, \boldsymbol{u}) + \boldsymbol{e}[\hat{\iota} + 2\omega\zeta(y - \hat{\tau}_1)], \quad \hat{\boldsymbol{x}}_\tau(0) = \hat{\boldsymbol{x}}_{\tau o} \quad (11b)$$

$$\dot{\hat{\iota}} = \omega^2(y - \hat{\tau}_1), \qquad \hat{\iota}(0) = \hat{\iota}_0 \quad (11c)$$

$$\boldsymbol{\chi} = \boldsymbol{g}(\hat{\boldsymbol{x}}_c, \hat{\boldsymbol{x}}_\tau, \boldsymbol{u}), \qquad \dim \boldsymbol{x} = n \quad (11d)$$

where

$$n = 3N + 1, \qquad N \le N_q = 20 \quad (11e)$$

$$\boldsymbol{e} = (1,0,\dots 0)^T, \quad \boldsymbol{x}_e = (\boldsymbol{x}_c^T, \boldsymbol{x}_\tau^T, \hat{\iota})^T \quad (11d)$$

$$\zeta \approx 1.5, \qquad \omega \approx n_\omega \lambda_c, \qquad n_\omega \in [10, 30] \quad (11f)$$

ζ (or ω) is the damping factor (or characteristic frequency) of the prescribed output error dynamics, λ_c is inverse of the reactor settling time. The integral action (with state $\hat{\iota}$): (i) compensates the modeling error (ι) of the temperature dynamics at the (most sensitive) measurement stage, where most of the exothermic reactions occur, and (ii) asymptotically cancels (in a practical sense) the output prediction error.

4.3 Estimator functioning

Define the (weighted transient ε^t plus SS ε^{ss}) errors ε_m (12a) of the $N_q(=20)$-stage model with perturbed parameter $(\mathrm{p} + \tilde{\mathrm{p}})$, and ε_N of the N vs N_q-stage model with nominal parameter (p).

$$\varepsilon_m = w_t \varepsilon_m^t + w_s \varepsilon_m^{ss}, \quad \varepsilon_N = w_t \varepsilon_N^t + w_s \varepsilon_N^{ss} \qquad (12a\text{-}b)$$

In other words, due to (typical and inexorable) kinetics-transport parameter errors, the staged models with $N_q = 20$ and $N_{fd} = 200$ (numerical PDE solver) describe the reactor experimental data equally well. The adjustable speed-stage number parameter pair $(n_\omega, N_e) = (10, 8)$ of the nonlinear estimator (11) is tuned as follows:

Step 1. Compute the error ε_m of the *N_q-stage model.*
Step 2. Fix the speed parameter at $n_\omega = 10$. Starting with a sufficiently small $N < N^-$, gradually increase N until the bistability property is described and the error ε_N (12a) is equal or smaller than ε_m (12b) at N_e.
Step 3. Increase the speed parameter n_ω and ratify or rectify its initial trial $n_\omega = 10$.

Fig. 6 presents the estimator functioning

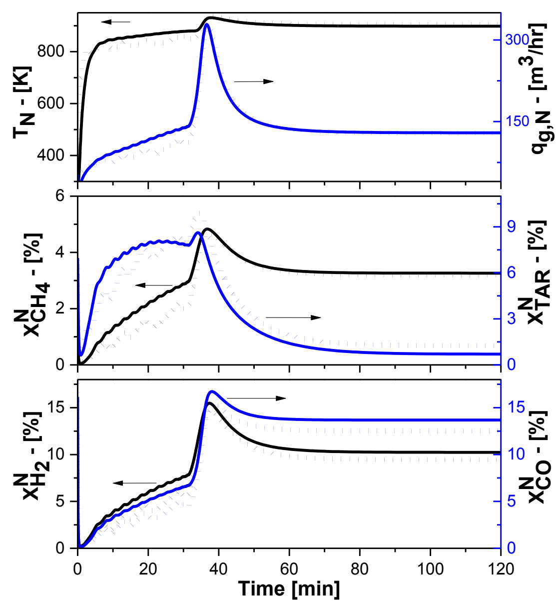

Fig. 6. Functioning of the geometric estimator (11) with $(\zeta, n_\omega, N_e^q) = (1.5, 10, 8)$, for the startup of the syngas tubular reactor. Estimated (discontinuous plots) and actual (continuous plots, generated with $N = N_q = 20$) effluent temperature (T_N), gas flow (q_g^N), as well as methane ($x_{CH_4}^N$), TAR (x_{TAR}^N), hydrogen ($x_{H_2}^N$), and carbon monoxide (x_{CO}^N) concentrations.

Overall, the results are good: with $\varepsilon_N^t = IAE_T$ (or ε_N^{ss}) of $16.78\,°C$ (or $6.71\,°C$) for temperature, $7.83\, m^3/hr$ (or $0.45\, m^3/hr$) for syngas flow and an average of $0.73\%V/V$ (or $0.56\%V/V$) for all gas component molar fractions. The SS estimation errors are: (i) less than 2% for temperature (T), flow (q_g) and methane (CH_4) concentrations, (ii) 7 and 9% for hydrogen (H_2) and carbon monoxide (CO) concentrations and (iii) as expected (due to kinetic function error), of 37% for tar concentration.

6. CONCLUSIONS

The problem of designing an application-oriented robustly convergent state estimator for the distributed syngas reactor has been solved with a geometric estimator that has considerably less ODEs than the ones of the nonlinear EKF technique.

The design has a systematic construction and a tuning procedure for the gain-stage number pair. The estimation error with 8 stages is comparable with the one of the 20-stage model with typical parameter errors. Thus, the injection of a single-temperature measurement at the most sensitive position enabled a model reduction of 12 stages.

The proposed observer design is a point of departure to study: (i) the estimation problem with more sensors to compensate unmeasured feed disturbances, (ii) the design of an output-feedback control scheme, and (iii) the design of off-line and on-line model calibration schemes.

REFERENCES

Alvarez, J., Fernandez, C. (2009). Geometric estimation of nonlinear process systems, Journal of Process Control, 19 (2), 247–260.

Andronov, A. A., & Pontryagin, L. S. (1937). Systémes grossiéres. Dokl. Acad. Nauk SSSR, 14, 247 – 251.

Amundson N. R. (1980), The Mathematical Understanding of Chemical Engineering Systems, Pergamon, 6, 493-631

Badillo-Hernandez, U., Alvarez-Icaza, L., & Alvarez, J. (2013). Model design of a class of moving-bed tubular gasification reactors. Chemical Engineering Science, 101, 674 – 685.

Badillo-Hernandez, U., Alvarez, J. & Alvarez-Icaza, L. (2016). Modeling the global nonlinear dynamics of tubular gasification reactors. In preparation to be submitted to Chemical Engineering Science.

Bashir, S., Chovln, T., Masri, B. J., Mukherjee A., Pant A., Sen S., and Vijayaraghavan P., (1992). Thermal Runaway Limit of Tubular Reactors, Defined at the Inflection Point of the Temperature Profile. Ind. Eng. Chem. Res., 31, 2164-2171.

Botero, H., Alvarez, H., Gómez, L. (2013) Estimación de Estado y Control de un Gasificador de Carbón en Lecho Fluidizado Presurizado, Revista Iberoamericana de Automática e Informática Industrial RIAI, 10 (3), 279-290.

Ciccarella, G., Dalla Mora, M. & Germani, A. (1993) A Luenberguer-like observer for nonlinear systems, Int. J. Contr. 57 (3) 537–556.

Deans, H. A., & Lapidus, L. (1960). A computational model predicting and correlating the behavior of fixed bed reactors: II Extension to chemically reactive systems. AIChE Journal, 6, 663–668.

Deckwer, W.-D. (1974). The backflow cell model—applied to nonisothermal reactors. The Chemical Engineering Journal, 8, 135 –144.

Dhooge, A., Govaerts, W., & Kuznetsov, Y. A. (2003). Matcont: A matlab package for numerical bifurcation analysis of odes. ACM Trans. Math. Softw., 29, 141–164.

Di Blasi, C. (2000). Dynamic behaviour of stratified downdraft gasifiers. Chemical Engineering Science, 55, 2931–2944.

Dochain, D., Perrier, M., Ydstie, B., (1992). Asymptotic observers for stirred tank reactors. Chemical Engineering Science, 47, 4167–4177.

Fernandez, C., Alvarez, J., Baratti, R., and Frau, A. (2012). Estimation structure design for staged systems. *Journal of Process Control*, 22 (10), 2038-2056.

Gauthier, J.P., H. Hammouri & S. Othman, S. (1992) A simple observer for nonlinear systems applications to bioreactors, IEEE Trans. Automat. Contr. 37 (6) 875–880.

Gelb, A. Applied Optimal Estimation, MIT Press, Cambridge, Massachusetts, 1974.

Gobel, B., Henriksen, U., Jensen, T. K., Qvale, B., & Houbak, N. (2007). The development of a computer model for a fixed bed gasifier and its use for optimization and control. Bioresource Technology, 98, 2043 – 2052.

Hlavacek, V. (1970). Aspects in design of packed catalytic reactors. Industrial & Engineering Chemistry, 62(7), 826.

Kazantzis, N. and Kravaris, C. (2000). Nonlinear observer desing for process monitoring. Industrial & Engineering Chemical Research, 39,408-419.

Kuznetsov, Y. A. (1998). Elements of Applied Bifurcation Theory. Springer.

Levenspiel, O. (1962). Chemical reaction engineering: an introduction to the design of chemical reactors. John Wiley and Sons.

Malkow, T. (2004). Novel and innovative pyrolysis and gasification technologies for energy efficient and environmentally sound MSW disposal. Waste Management, 24, 53 – 79.

Milligan, J. B. (1994). Downdraft gasification of biomass. PhD Thesis, Aston University

Nájera, I., Álvarez, J., Baratti, R., Gutiérrez, C. (2016) Control of an exothermic packed-bed tubular reactor, IFAC-PapersOnLine, 49(7), 278-283

Porru, M., Alvarez, J. & Baratti, R. (2013) Composition estimation design for industrial multicomponent column Chemical Engineering Transactions 32, 1975-1980

Ranzi, E., Corbetta, M., Manenti, F., & Pierucci, S. (2014). Kinetic modeling of the thermal degradation and combustion of biomass. Chemical Engineering Science, 110, 2 – 12. Mackie-2013 “Pushing the boundaries”.

Shinnar, R. (1986). Use of residence- and contact-time distributions in reactor design. Chemical reaction and reactor engineering, Editors: James J. Carberry and Arvind Varma, 1, 63–150.

Shwe, S. (2004). A theoretical and experimental study on a stratified downdraft biomass gasifier. PhD Thesis, University of Melbourne, Australia.

Varma, A. (1980). On the number and stability of steady states of a sequence of continuous-flow stirred tank reactors. Industrial and Engineering Chemistry Fundamentals, 19, 316–319.

Wilson, J.A., Chew, M. & Jones, W.E. (2006). State estimation-based control of a coal gasifier. IEE Proceedings Control Theory and Applications, 153, 270–276.

Zeitz, M. (1987) The extended Luenberger observer for nonlinear systems, Syst. Contr. Lett. 9 (2) 149–156.